Application of C-COM for Microwave Integrated-Circuit Modeling

Kang Lan, *Member, IEEE*, Sujeet K. Chaudhuri, *Senior Member, IEEE*, and S. Safavi-Naeini, *Member, IEEE*

***Abstract*—The concurrent complementary operators method (C-COM) is extended to simulate microwave planar circuits with the finite-difference time-domain (FDTD) method for the first time. The dispersive boundary condition (DBC) and its complementary operator are used to truncate the FDTD lattices and the fields in the boundary layers are calculated, respectively. Then these two simulations are averaged to annihilate the first-order reflections. Numerical error analysis shows that the performance of the DBC is improved greatly due to the implementation of complementary operators, and the setup of its parameters becomes easier and more robust. A flexible and high-performance absorbing boundary condition is thus obtained through the combination of the DBC and C-COM. This method has been successfully used to simulate a variety of planar circuit structures. Simulations of a microstrip low-pass filter, coupled-line bandpass filter, modified microstrip transmission lines, and dielectric resonator antenna, are presented in this paper.**

***Index Terms*—Absorbing boundary conditions (ABCs), dielectric antennas, finite-difference time-domain (FDTD) methods, microwave circuits.**

I. Introduction

FLEXIBLE and high-performance absorbing boundary conditions (ABCs) are required to obtain high efficiency of the finite-difference time-domain (FDTD) method for unbounded space problems. The complementary operators method (COM) has proven to be a very good ABC [1]–[3] for free-space problems. This method uses two complementary boundary operators whose reflection coefficients are identical in magnitude, but opposite in sign. The first-order reflections from the truncated boundary are cancelled by performing two independent simulations. In the concurrent scheme of this method, termed the concurrent complementary operators method (C-COM) [4], the two complementary operators are employed concurrently in the same simulation, thus the computation is reduced by about one-half.

The complementary concept, in which two independent simulations with different boundary conditions are executed, has been applied in several previous ABCs to reduce the errors. In the superabsorbing technique [6], the ABC is applied both to the nodes along the termination layers of the computation domain and to interior nodes adjacent to the termination. From these two applications of the ABC, an error term is estimated and used to correct the values at the termination layers of the computation domain. However, this method can only reduce the reflection for traveling waves [2]. In the geometry rearrangement technique [7], the dominant reflection from the ABC is corrected by superposition of two subproblems with different sources or boundary locations. The method can be used to estimate and correct the imperfect absorption of the ABC both for traveling and evanescent waves. However, this method can be used only for guided-wave problems, and only reflections from far and near ends of the waveguides can be cancelled. In the C-COM, the errors caused by the first-order reflection for traveling waves and evanescent waves can be annihilated completely in any directions, and the errors will only depend on the second-order reflections [2]. If a high-performance ABC is used as the fundamental operator, the errors will be very small. Thus, the focus of applying the C-COM is to find a high-performance ABC with an available complementary operator, i.e., a pair of ABCs with complementary (opposite) reflection.

Using Higdon's ABC [8] as the fundamental operator, the C-COM has been utilized to simulate free-space problems such as the radiation from line sources, scattering from perfect conducting cylinders [2]–[4], and waveguiding structures [5]. In this paper, we will extend this method to arbitrary multilayer microwave structures. In Higdon's ABC, the waves are assumed to travel with the same speed and different incidence angles toward the boundary plane. For the guided-wave problems of interested to this study, we cannot directly use the algorithm in [2]–[4] since, in Higdon's operator, there is the fundamental assumption of a uniform wave speed in the formulation. When a Gaussian pulse travels in guided-wave structures, the velocities of fields are different for the different frequency component of the pulse due to the dispersion property of these structures. Based on this fact, to configure the complementary operator, we use the dispersive boundary condition (DBC) [9], [10] that can absorb waves over a reasonably wide frequency band. The parameters in the DBC can be set to absorb waves with different velocities, including the evanescent waves [9]. Techniques to select these parameters have also been studied. It has been shown that the DBC can obtain good absorption by optimizing the parameters [11]–[14]. In this paper, we will show that, through the utilization of complementary operators, the performance of the DBC will be further improved, and the setting of those parameters will be more flexible.

The complementary operators for the DBC and the concurrent implementation are presented briefly in Section II. In Section III, criteria for the selection of parameters are given and numerical error analysis is implemented to study the performance of the complemented DBC. Application

Manuscript received December 9, 2002.

The authors are with the Department of Electrical and Computer Engineering, University of Waterloo, Waterloo, ON, Canada N2L 3G1 (e-mail: klan@maxwell.uwaterloo.ca; sujeet@maxwell.uwaterloo.ca; safavi@maxwell.uwaterloo.ca).

Digital Object Identifier 10.1109/TMTT.2003.809635

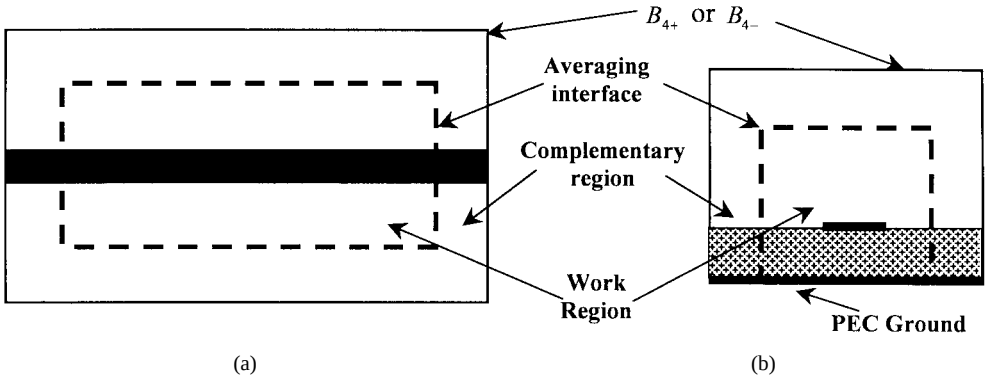

Fig. 1. C-COM for a microstrip transmission line. (a) Top view. (b) End view.

examples, including a microstrip low-pass filter, coupled-line bandpass filter, a modified microstrip transmission lines, and a microstrip-fed dielectric-resonator antenna, are presented in Section IV. Finally, conclusions are given in Section V.

II. Complemented DBC

A. Complementary Operators: B_{4+} and B_{4-}

The Mth-order DBC is expressed as [9]

$$[\mathrm{DBC}_M]\Phi = 0 \tag{1}$$

where $\mathrm{DBC}_M = \prod_{i=1}^{M}(\partial/\partial x + (\beta_i/c)(\partial/\partial t) + \alpha_i)$, c is the speed of light, $\overline{\beta} = \{\beta_1, \beta_2, \ldots, \beta_M\}$, and $\overline{\alpha} = \{\alpha_1, \alpha_2, \ldots, \alpha_M\}$ are parameters to be set. The associated theory reflection coefficient is given by

$$\Gamma_M = -\prod_{i=1}^{M} \frac{-j\gamma_x + j\beta_i k + \alpha_i}{j\gamma_x + j\beta_i k + \alpha_i} \tag{2}$$

where γ_x is the complex wavenumber of the incidence wave.

Suppose $\alpha_M = 0$, (2) is then rewritten as

$$\Gamma_M = \frac{-j\gamma_x + j\beta_M k}{j\gamma_x + j\beta_M k}\Gamma_{M-1} \tag{3}$$

and (1) becomes

$$\left[\left(\frac{\partial}{\partial x} + \frac{\beta_M}{c}\frac{\partial}{\partial t}\right)\mathrm{DBC}_{M-1}\right]\Phi = 0. \tag{4}$$

Since for boundary condition $((\partial/\partial x) + (\beta_M/c)(\partial/\partial t))\Phi = 0$ is equal to $((c/\beta_M)(\partial/\partial x) + \partial/\partial t)\Phi = 0$, from (4), we have

$$\begin{cases} \left[\dfrac{\partial}{\partial x}\mathrm{DBC}_{M-1}\right]\Phi = 0, & \beta_M \Rightarrow 0 \\ \left[\dfrac{\partial}{\partial t}\mathrm{DBC}_{M-1}\right]\Phi = 0, & \beta_M \Rightarrow \infty. \end{cases} \tag{5}$$

The corresponding reflection coefficients are obtained from (3)

$$\Gamma_M = \begin{cases} -\Gamma_{M-1}, & \beta_M \Rightarrow 0 \\ \Gamma_{M-1}, & \beta_M \Rightarrow \infty \end{cases} \tag{6}$$

which indicates that the pairs of operators in (5) are complementary.

The application of complementary operators can only annihilate the first-order reflections [2]–[4], thus, higher order operators should be considered to minimize the second-order reflections. In practice, however, very high orders cannot improve the accuracy and, on the contrary, make the solution instable. Although the loss term $\overline{\alpha}$ can be used to circumvent this shortcoming, it is not effective if M is too large. At the same time, if $\overline{\alpha}$ is increased substantially in order to stabilize the solution, the accuracy of low-frequency responses will be reduced. After considering these factors, we choose $M = 4$, and represent the complementary operators as

$$B_{4+} = \frac{\partial}{\partial x}\mathrm{DBC}_3 \tag{7}$$

$$B_{4-} = \frac{\partial}{\partial t}\mathrm{DBC}_3. \tag{8}$$

B_{4+} and B_{4-} have same theoretical reflection coefficients as DBC_3 in magnitude, although they have higher order derivatives. If B_{4+} or B_{4-} are used as the ABC independently, there are no improvements compared with DBC_3. However, it will be shown that the reflections can be suppressed greatly as B_{4+} and B_{4-} are used as complementary operators.

B. Concurrent Implementation: C-COM

If the FDTD results with computation domain truncated by B_{4+} and B_{4-} are $\Phi^{(B_{4+})}$ and $\Phi^{(B_{4-})}$, respectively, the final solution is obtained by [2], [3]

$$\Phi = \frac{1}{2}\left(\Phi^{(B_{4+})} + \Phi^{(B_{4-})}\right). \tag{9}$$

We can compute the fields in the whole computation domain two times using B_{4+} and B_{4-}, respectively, then use the average of the two simulations to update the fields in the next FDTD time march [2], [3]. This scheme will require approximately double the time that would be needed to solve the same problem with the corresponding DBC_3. In order to overcome this problem, the concurrent scheme [4] is applied.

Fig. 1 demonstrates this scheme for a microstrip transmission line. The complete computation domain is divided into a work region and complementary region. Within the work region, each of the field components is computed once. However, within the complementary region, each of the field components is assigned two storage locations and each set of field components are updated independently using B_{4+} or B_{4-} as the ABC. The field values on the interface, which will be used to update the field components in the work region at the next step, are obtained by averaging the two sets of field values obtained in the complementary region.

In order to demonstrate the mechanism of complementary operators, Fig. 2 gives the computation errors for the currents' re-

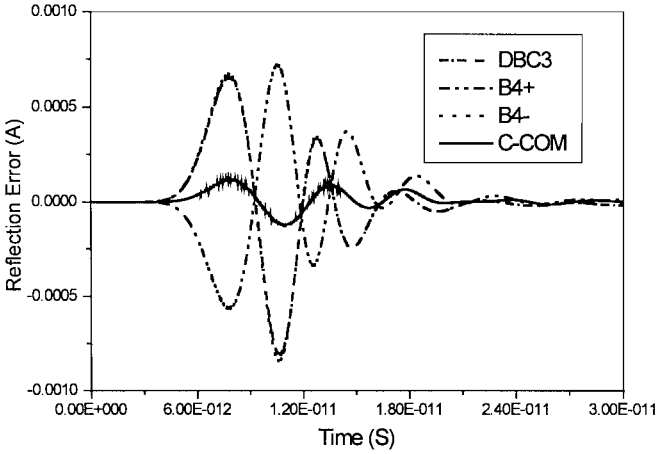

Fig. 2. Computation errors for the current of a microstrip transmission line. The width of the transmission line is 75 μm. The height and dielectric constant of the substrate are 100 μm and 13.0. FDTD cells sizes are $\Delta x = \Delta y = \Delta z = 6.25$ μm.

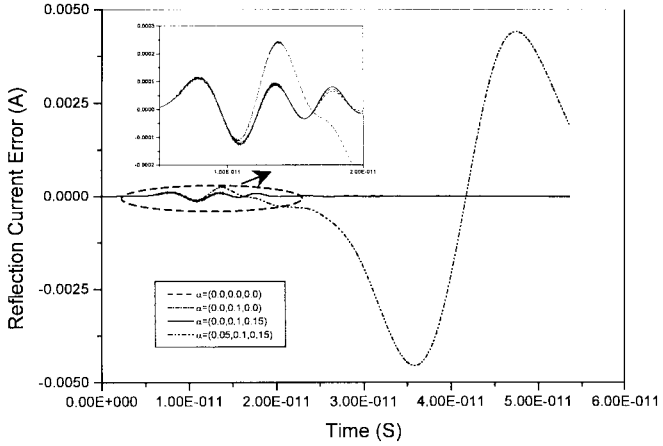

Fig. 3. Current of the microstrip given in Fig. 2, simulated by the C-COM with a different loss term for faces at the far and near ends.

flection error on a microstrip transmission line at each time step computed by different methods. The distances between the microstrip edges and the left and right truncation faces' near and far ends are 20 cells. The number of boundary layers is ten for the C-COM so the distance between its interface and the edges of the microstrip is ten cells. The distance between the surface of the microstrip and the top truncation face is 12 cells, hence, there are only two cells between the interface of the C-COM and the surface of the microstrip. In the boundary conditions, $\overline{\beta^2} = \{8.5, 9.0, 9.5\}$, $\overline{\alpha} = \{0.05, 0.1, 0.15\}$ for the top, left, and right truncation faces, and $\alpha = \{0.0, 0., 0.0\}$ for the faces at the near and far ends. The selection of these parameters will be discussed in Section III.

It is observed from Fig. 2 that, as predicated in (6), the reflection of DBC_3 is almost the same as B_{4-}, and the reflection of B_{4+} is almost identically opposite, i.e., $\Gamma_{\mathrm{DBC3}} \approx \Gamma_{B4-} \approx -\Gamma_{B4+}$. The reflection of the C-COM is almost the average of reflections of B_{4+} and B_{4-}. The errors in the C-COM come from the second-order reflections, especially from the corners of the computation domain.

III. Parameter Setup and Error Analysis

In this section, we will discuss the selection of parameters in the boundary conditions. The performance of the complemented DBC will also be discussed.

A. Parameter Setup

The parameters in the boundary conditions include $\overline{\beta}$, $\overline{\alpha}$, and the number of boundary layers. The velocities and attenuations of waves propagating in different directions may be different. Hence, in our program, parameters for different truncation faces can be set individually according to the properties of the impinging waves.

An estimated $\overline{\beta}$ for microwave planar circuits is [9]

$$\overline{\beta} = \{\beta_i|_{i=1,2,3}\} = \left\{ \sqrt{\varepsilon_{\mathrm{reff}}(f_i)}\Big|_{i=1,2,3} \right\} \qquad (10)$$

where $\varepsilon_{\mathrm{reff}}$ is the effective dielectric constant, which is a function of frequency. Generally, for a structure to be simulated, $\varepsilon_{\mathrm{reff}}$ is unknown. For DBCs, several techniques to set optimal $\overline{\beta}$ have been discussed in [11]–[14]. As shown in [9], if higher orders are used, $\varepsilon_{\mathrm{reff}}$ can be selected over a wide range between the static solution and the exact dielectric constant of the structure. We will show that, especially if complemented operators are used, $\overline{\beta}$ can be selected in a wide range, and the results are robust. Hence, another advantage of applying the complementary operators is that the restrictions on the selection of parameters are relaxed.

$\overline{\alpha}$ is used to simulate the attenuations of waves, and to steady the solutions since high-order derivatives in the ABC are used. $\overline{\alpha}$ can also be used to absorb the evanescent waves [9]. The additional derivatives in space and time in order to obtain B_{4+} and B_{4-} from DBC_3, as shown in (7) and (8), will increase the risks of instabilities. After treating the boundary condition carefully with double precision, the solution of DBC_3 can be robust for very small values of $\overline{\alpha}$, even zeros [9]. However, it is found that B_{4+} and B_{4-}, especially B_{4+}, tend to diverge after a longer time marching if $\overline{\alpha}$ is set to zero or very small values due to the additional derivatives compared with DBC_3. On the other hand, $\overline{\alpha}$ cannot be too large. Large values of $\overline{\alpha}$ will reduce the accuracy of low-frequency responses and increase the reflections from the boundaries. Thus, $\overline{\alpha}$ should be set as small as possible as long as the solution is stable. Fortunately, we found that typical values such as $\overline{\alpha} = \{0.05, 0.1, 0.15\}$ are applicable for many structures we have studied.

An important requirement for the setup of $\overline{\alpha}$ is that it must have at least one zero element for truncation faces at the far and near ends of a transmission line, otherwise reflections from these faces will be large. This is because the attenuation of the principle propagation mode impinging on these faces is very small. Fig. 3 presents the simulated current error on the microstrip given in Fig. 1 with dimensions given in the caption of Fig. 2. The parameters in the boundary condition are the same as used for the analysis in Fig. 2, except a different loss term $\overline{\alpha}$ is used for the faces at the near and far ends. It is seen that, as long as $\overline{\alpha}$ has at least one zero-element, the effect of using different element values is very small. However, for $\overline{\alpha} =$

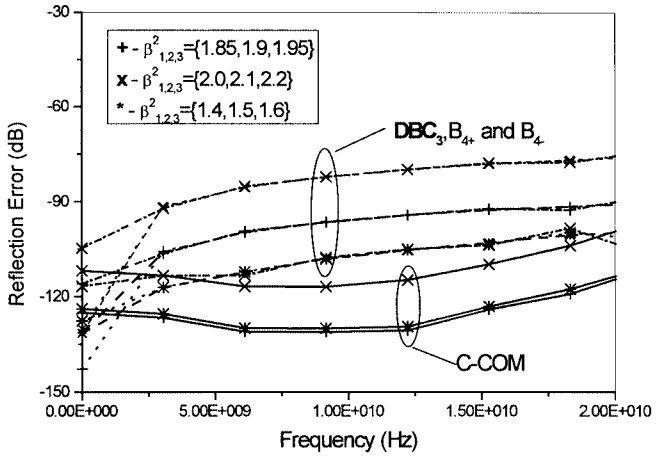

Fig. 4. Reflection error of a shielded microstrip line with a width of 0.254 mm, substrate height of 0.254 mm, and $\varepsilon = 2.2$. The top of the perfect electric conductor (PEC) enclosure is at 0.762 mm from the substrate, and the distance between the edges of the microstrip and PEC walls is 0.928 mm. The cell sizes are $\Delta x = \Delta y = 0.042\,333$ mm and $\Delta z = 2\Delta x$.

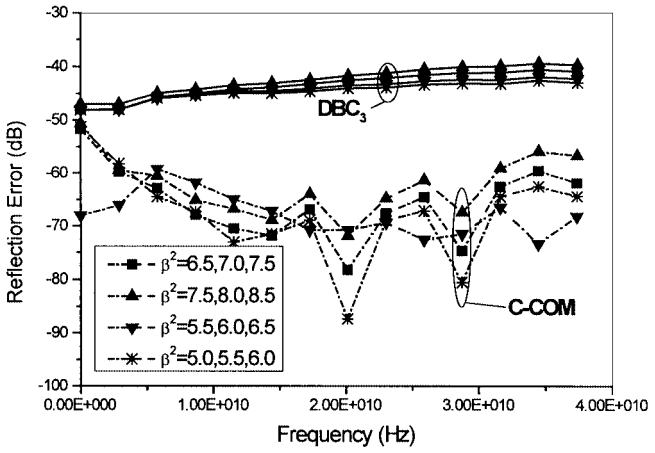

Fig. 5. Reflection error of a microstrip line with a width of 0.254 mm, substrate height of 0.254 mm, and $\varepsilon_r = 9.8$. The cell sizes are the same as Fig. 4.

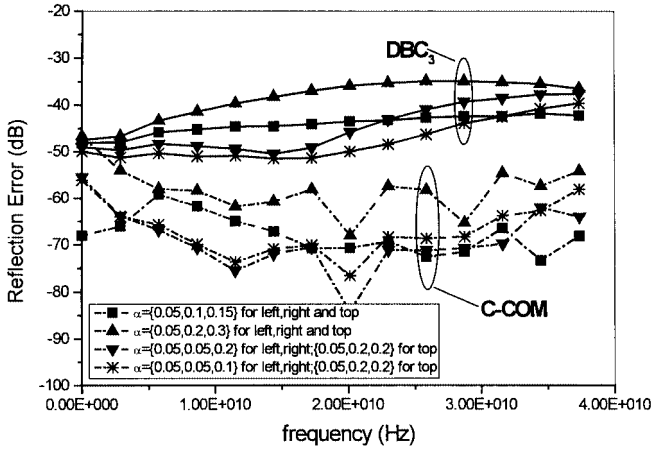

Fig. 6. Reflection error of the microstrip line given in Fig. 5.

$\{0.05, 0.1, 0.15\}$, the reflections from the ends become hazardous after the incidence waves reach the two faces. Hence, we always set $\overline{\alpha} = \{0.0, 0.0, 0.0\}$ for faces at the ends of a transmission line: input and output ports of a microwave component.

B. Numerical Error Analysis

In order to study the effect of parameters in the boundary conditions, reflections for a shielded microstrip are studied first. The reflection errors for frequencies up to 20 GHz calculated by DBC_3, B_{4+}, and B_{4-}, and the C-COM with ten boundary layers are given in Fig. 4. The microstrip is shielded so the terminating effects of ends can be studied. Since only the propagating waves exist, $\overline{\alpha}$ is set to zero. It is shown again in Fig. 4 that DBC_3, B_{4+}, and B_{4-} have almost the same absorption performances. The effective dielectric constant of this strip line is $\varepsilon_{\mathrm{reff}} = 1.76$, however, we can see that, even if the parameters have a large variation around this value, the absorption performance is still very good for DBC_3, B_{4+}, and B_{4-} because of their higher order [9] and only the ends need to be terminated. The great improvement in accuracy is obtained with the use of complementary operators. Also, the influence of the parameter values on the results will be even smaller. Thus, $\overline{\beta}$ can be set around the square root of the static effective dielectric constant $\varepsilon_{\mathrm{reff}}$ and can be varied up to substrate dielectric constant ε_r without affecting the simulation accuracy.

Since B_{4+}, B_{4-}, and DBC_3 have similar absorption properties, only DBC_3 will be used as the comparison with the C-COM in the following calculations.

A uniform microstrip transmission line without a shield is simulated in Figs. 5 and 6. The distances from the boundary truncation faces to the edges and surface of the microstrip are 20 cells. Ten boundary layers are used in the C-COM. Fig. 5 demonstrates the effect of $\overline{\beta\alpha} = \{0.05, 0.1, 0.15\}$ with fixed $\overline{\alpha} = \{0.05, 0.1, 0.15\}$ for the top, left, and right truncation faces. $\overline{\alpha}$ is set to zero for truncation faces at the near and far ends. The static effective dielectric constant of this microstrip line is approximately 6.58. With a series of $\overline{\beta} = \{\beta_1, \beta_2, \beta_3\}$ with element values changed widely from $\sqrt{5}$ to $\sqrt{8.5}$, the average variation of reflections are seen to be within 5 dB.

With $\overline{\beta^2}$ fixed at $\{5.5, 6, 6.5\}$, reflection errors for four sets of $\overline{\alpha}$ values are compared in Fig. 6. As we have pointed out, for faces at the near and far ends of a transmission line, there should be at least one zero element in $\overline{\alpha}$. Hence, we set $\overline{\alpha} = \{0.0, 0.0, 0.0\}$ for the faces at both ends. For other faces, based on numerical trials, we found that the average of $\{\alpha_1, \alpha_2, \alpha_3\}$ should be no less that 0.1, otherwise the increasing reflections will tend to produce a diverging solution. It is found that, as $\overline{\alpha}$ is set to very large values, 0.2 or above, for example, the reflection errors for DBC_3 will be larger than -40 dB. However, the reflection errors for the C-COM can still be kept lower than -65 dB unless very large values are used for $\overline{\alpha}$, 0.3, or above, for example. Hence, the C-COM is more insensitive to the parameters than DBC_3, which allows for a more flexible parameter setup.

Finally, the number of boundary layers should be no less than five [4]. Increasing the number of boundary layers require additional storage and computation. Numerical tests show that, for the simulation of the shielded microstrip line given in Fig. 4, with almost no evanescent waves, the difference between using five and ten layers is less than 1 dB. For the microstrip line described in Fig. 5, which has evanescent waves, increasing the

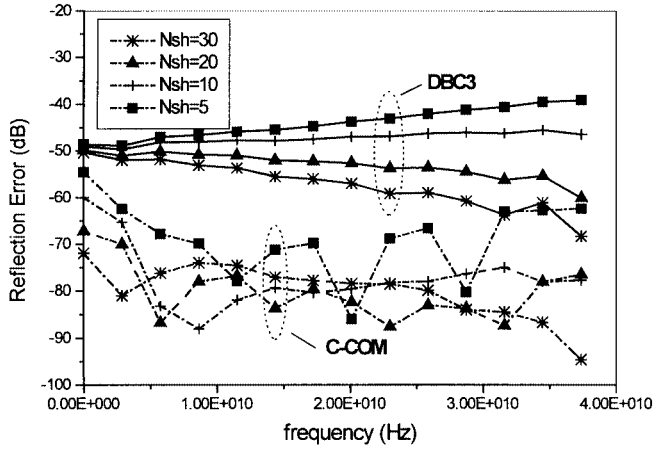

Fig. 7. Reflection error of the same microstrip line given in Fig. 5. $\overline{\alpha} = \{0.05, 0.1, 0.15\}$ for the top, left, and right truncation faces, $\overline{\alpha} = \{0.0, 0.0, 0.0\}$ for truncation faces at the two ends of the microstrip. $\overline{\beta^2} = \{6.5, 7.0, 7.5\}$.

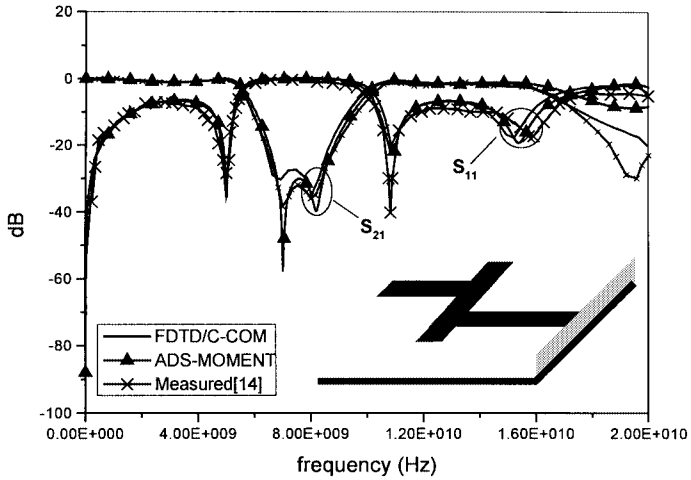

Fig. 8. Microstrip low-pass filter. The dielectric constant of the substrate is $\varepsilon_r = 2.2$ and the height of the substrate is 0.794 mm. The width of the cross branch is 2.54 mm. The width of the input and output port is 2.413 mm, and their symmetric central line to the center of the cross branch is 3.034 mm. $\Delta x = 0.406$ mm, $\Delta y = 0.423$ mm, and $\Delta z = 0.265$ mm.

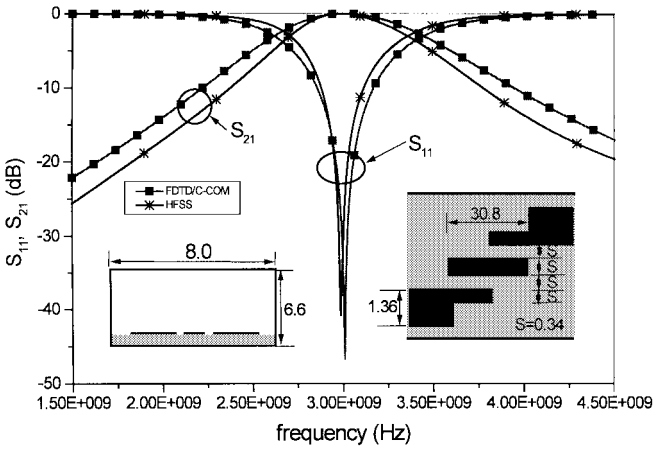

Fig. 9. Return and insertion losses of a bandpass filter. The dielectric constant of the substrate is 3.45 and the thickness is 0.6 mm. The sizes of the circuits and shield are given in the plot. $\Delta x = 0.4$ mm, $\Delta y = 0.17$ mm, and $\Delta z = 0.2$ mm.

number of boundary layers will improve the performance of the C-COM. However, the average difference between using five and ten layers is approximately 3 dB. This means that 5–10 layers are sufficient to obtain good absorbing properties.

In order to study the effect of truncation positions of the C-COM, Fig. 7 compares reflections of the microstrip line given in Fig. 5 as the distance from the right edge of the microstrip to the right averaging interface of the C-COM that varies from 30 to five cells. The distance at another side is fixed at 30 cells, with ten boundary layers. We can see that, as the distance changed from 30 to ten cells, the reflection errors remained lower than -70 dB. Even as the distance reduced to five cells, the reflection from the C-COM boundary is still less than -60 dB. However, for DBC_3, the changes in reflections are very large, and potentially the reflections will be higher than -40 dB as the frequency is increased.

IV. Applications

We have applied the complemented DBC presented in this paper to simulate single-layer or multilayer microwave planar circuits and printed antenna problems.

Fig. 8 gives the frequency response of the microstrip low-pass filter presented in [15]. The result of Agilent *ADS Moment* is also given for comparison. We set $\overline{\alpha} = \{0.0, 0.0, 0.0\}$ for the truncation faces at the input and output ports, and $\overline{\alpha} = \{0.05, 0.1, 0.15\}$ for the top, left, and right truncation faces. $\overline{\beta^2} = \sqrt{\{1.6, 1.7, 1.8\}}$. Other values for $\overline{\beta}$ have been used, but the differences between the obtained results are negligible. The frequency response of this filter over 0–20 GHz has been given. In the FDTD simulation, the total mesh dimensions are $80 \times 70 \times 20$, and ten boundary layers are used for the C-COM. The simulation is performed for 5000 time steps and the computation time for this circuit is 57 min on a Pentium III 600-MHz personal computer.

In Fig. 9, the results for the return and insertion losses of a microstrip bandpass filter are compared with the Ansoft *HFSS* solutions. The effect of the shield is included in the simulation. Hence, only the input and output ends need to be terminated. The static effective dielectric constant without considering the effect of shielding is approximately 2.7, thus, we choose $\overline{\beta}\sqrt{\{2.5, 2.7, 2.9\}}$. $\overline{\alpha}$ is set to zero. The difference between the center frequency of the filter predicated by our method and Ansoft *HFSS* is approximated 0.8%.

Fig. 10 shows the effective dielectric constant and characteristic impedance for a modified multilayer microstrip line that is developed for high-quality RF integrated circuit (RFIC)/monolithic-microwave integrated-circuit (MMIC) transmission lines and inductors [16]. This kind of microstrip lines not only lowers the dissipative loss, but also enables the realization of very high characteristic impedance lines on thin high dielectric-constant substrates such as GaAs. Further improvement may be obtained by etching away the surrounding polyimide so that more of the microstrip is surrounded by air, as represented by "CASE II" in Fig. 10. The results are compared with the data from [16]. Setup for $\overline{\alpha}$ is the same as in Fig. 8. In order to obtain better absorption performance for different thicknesses, we have used dif-

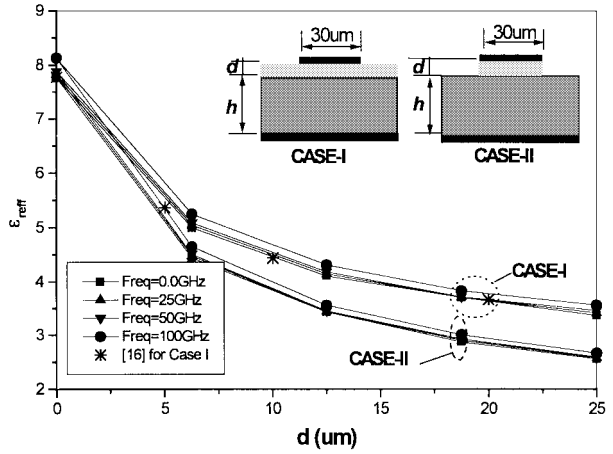

Fig. 10. Effective dielectric constant of a modified high-quality mutilayer microstrip line for an RFIC/MMIC. The width of the microstrip is 30 μm and the substrate has two layers. The height of the GaAs layer is $h = 75$ μm and $\varepsilon_{r\mathrm{GaAs}} = 12.9$. The dielectric constant for the polyimide layer is $\varepsilon_{r\mathrm{poly}} = 3.2$, its thickness d is changed from 0 to 25 μm. The cell sizes are $\Delta x = \Delta y = 6.0$ μm and $\Delta z = 6.25$ μm.

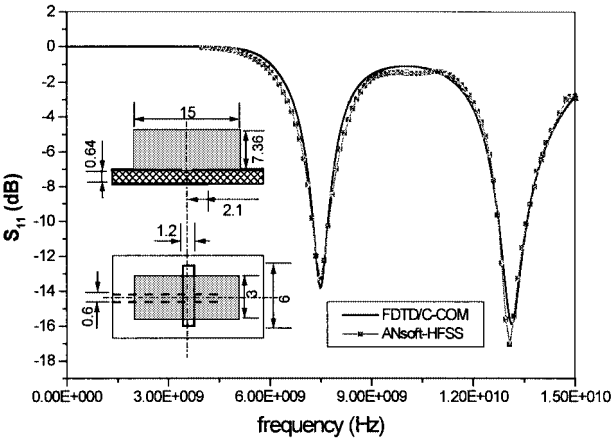

Fig. 11. Return loss of an aperture-coupled rectangular DRA. The dielectric constants for the substrate and dielectric resonator are 10.2 and 10.8, respectively. The unit of the sizes given in this figure is in millimeters and the initial sizes are from [17]. The cell sizes are $\Delta x = \Delta y = 0.3$ mm and $\Delta z = 0.32$ mm.

ferent set of parameters as $\overline{\beta^2} = \{7.5, 8.0, 8.5\}$, $\{5.5, 6.0, 6.5\}$, $\{3.5, 4.0, 4.5\}$, or $\{3.0, 3.5, 4.0\}$ since we know that the characteristics of the transmission lines will vary greatly as the thickness changed. In order to select these parameters, some estimated values, such as the values between $\sqrt{\varepsilon_{r\mathrm{GaAs}}}$ and $\sqrt{\varepsilon_{r\mathrm{ploy}}}$ weighted by the substrate thickness, are used first. The effective dielectric constants are then obtained by the FDTD method. If these constants are far from the values we have set in the C-COM, we can reset the boundary conditions and better absorption performance will be obtained.

A rectangular aperture-coupled dielectric-resonator antenna is simulated as the last example. The static effective dielectric constant is approximately 6.8, and $\overline{\beta^2} = \{5.8, 6.3, 6.8\}$ is used. In this example, $\overline{\alpha} = \{0.05, 0.1, 0.15\}$ for the left, right, top, bottom, and far end truncation faces; $\overline{\alpha} = \{0.0, 0.0, 0.0\}$ only for the truncation face at the input port. The structure and sizes (in millimeters) are given in Fig. 11. The return losses computed by the FDTD method and Ansoft *HFSS* are compared. Two resonant frequencies and bandwidths predicted by different methods match very well.

V. Conclusion

In this paper, by using the DBC as the fundamental operator, the C-COM [4] is extended to multilayer microwave planar circuits for the first time. Criteria for the selection of parameters in the boundary conditions are discussed. Error analysis is used to study the performance of the boundary condition. It is shown that the implementation of complementary operators makes the selection of parameters more flexible. For all of the structures we have studied, the average reflection errors can be smaller than -65 dB without any optimization of the parameters. This method has been successfully applied in this paper to simulate a variety of guided-wave structures such as the multilayer modified microstrip transmission lines, microstrip low-pass filter, coupled-line bandpass filter, and the dielectric-resonator antenna.

References

[1] A. Taflove, *Advances in Computational Electrodynamics: The Finite-Difference Time-Domain Method*, 2nd ed. Norwood, MA: Artech House, 1998.

[2] O. M. Ramahi, "Complementary operators: A method to annihilate artificial reflections arising from the truncation of the computation domain in the solution of partial differential equations," *IEEE Trans. Antennas Propagat.*, vol. 43, pp. 697–704, July 1995.

[3] ——, "Complementary boundary operators for wave propagation problems," *J. Computat. Phys.*, vol. 133, pp. 113–128, 1997.

[4] ——, "The concurrent complementary operators method for FDTD mesh truncation," *IEEE Trans Antennas Propagat.*, vol. 46, pp. 1475–1482, Oct. 1998.

[5] ——, "Application of the complementary boundary operators in the FDTD solution of planar and printed circuits problems," in *Proc. Progress in Electromagnetic Research Symp.*, Seattle, WA, July 24–28, 1995.

[6] K. K. Mei and J. Fang, "Superabsorption: A method to improve absorbing boundary conditions," *IEEE Trans. Antennas Propagat.*, vol. 40, pp. 1001–1010, Sept. 1992.

[7] K. Naishadham and X. P. Lin, "Minimization of reflection error caused by absorbing boundary condition in the FDTD simulation of planar transmission lines," *IEEE Trans. Microwave Theory Tech.*, vol. 44, pp. 41–46, Jan. 1996.

[8] R. L. Higdon, "Absorbing boundary conditions for difference approximations to the multidimensional wave equation," *Math. Comput.*, vol. 47, pp. 437–459, Oct. 1986.

[9] J. Fang, "Absorbing boundary conditions applied to model wave propagation in microwave integrated-circuits," *IEEE Trans. Microwave Theory Tech.*, vol. 42, pp. 1506–1513, Aug. 1994.

[10] Z. Bi, K. Wu, C. Wu, and J. Litva, "A dispersive boundary condition for microstrip component analysis using the FD-TD method," *IEEE Trans. Microwave Theory Tech.*, vol. 40, pp. 774–777, Apr. 1992.

[11] C. J. Railton, E. M. Daniel, D.-L. Paul, and J. P. McGeehan, "Optimized absorbing boundary conditions for the analysis of planar circuits using the finite difference time domain method," *IEEE Trans. Microwave Theory Tech.*, vol. 41, pp. 290–297, Feb. 1993.

[12] V. Betz and R. Mittra, "Comparison and evaluation of boundary conditions for the absorbing of guided waves in an FDTD simulation," *IEEE Microwave Guided Wave Lett.*, vol. 2, pp. 499–501, Dec. 1992.

[13] C. R. Railton, E. M. Daniel, and J. P. McGeehan, "Use of second order absorbing boundary conditions for the termination of planar waveguides in the FDTD method," *Electron. Lett.*, vol. 29, pp. 900–902, May 1993.

[14] F. Moglie, R. Rozzi, and R. Severini, "Discontinuities in planar millimeter circuits by FD-TD method," in *2nd Int. Computation in Electromagnetics Conf.*, 1994, pp. 327–330.

[15] D. M. Sheen, S. M. Ali, M. D. Abouzahra, and J. A. Kong, "Application of the three-dimensional finite-difference time-domain method to the analysis of planar microstrip circuits," *IEEE Trans. Microwave Theory Tech.*, vol. 38, pp. 849–857, July 1990.

[16] I. J. Bahl, "Application notes: High- Q and low-loss matching network elements for RF and microwave circuits," *IEEE Microwave Mag.*, vol. 1, pp. 64–73, Sept. 2000.

[17] Y. M. M. Antar and Z. Fan, "Theoretical investigation of aperture-coupled rectangular dielectric resonator antenna," *Proc. Inst. Elect. Eng.*, pt. H, vol. 143, pp. 113–118, April 1996.

Kang Lan (M'00) received the B.S.E.E., M.E., and Ph.D. degrees in electrical engineering from the University of Electronic Science and Technology of China (UESTC), Chengdu, China, in 1992, 1995, and 1999, respectively.

From February 1997 to December 1999, he was with the Wireless Communication Research Center, City University of Hong Kong, as a Research Assistant and Senior Research Assistant, respectively. From December 1999 to March 2001, he was a Post-Doctoral Research Fellow with the MMIC and Packaging Laboratory, Department of Electrical and Computer Engineering, National University of Singapore. In March 2001, he joined the Department of Electrical and Computer Engineering, University of Waterloo, Waterloo, ON, Canada, where he is currently a Research Assistant Professor. His research interests include simulation and design techniques for RF/microwave passive circuits and antennas, active device characterization techniques for RF integrated circuit (RFIC)/MMIC design. His current research activities include compact and wide-band antenna design for mobile and wireless data communications, multilayer circuits for three-dimensional (3-D) RFICs/MMICs, and wireless system design.

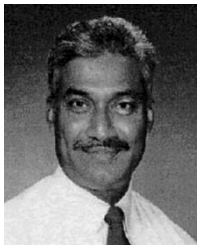

Sujeet K. Chaudhuri (M'79–SM'85) was born in Calcutta, India, on August 25, 1949. He received the B.E. degree (with honors) in electronics engineering from the Birla Institute of Technology and Science (BITS), Pilani, India, in 1970, the M.Tech. degree in electrical communication engineering from the Indian Institute of Technology (IIT), Delhi, India, in 1972, and the M.A.Sc. degree in microwave engineering and Ph.D. degree in electromagnetic theory from the University of Manitoba, Winnipeg, MB, Canada, in 1973 and 1977, respectively.

In 1977, he joined the University of Waterloo, Waterloo, ON, Canada, where he is currently a Professor in the Electrical and Computer Engineering Department and former Chair of the Electrical and Computer Engineering Department (1993–1998). He was also a Visiting Associate Professor with the Electrical Engineering and Computer Science Department, University of Illinois at Chicago (1981, 1984) and the National University of Singapore (1990–1991). He has been involved in contract research and consulting work with several Canadian and U.S. industries and government research organizations. His current research interests are guided-wave/electrooptic structures, planar microwave structures, dielectric resonators (DRs), optical and electromagnetic imaging, and fiber-based broad-band networks.

Dr. Chaudhuri is a member of URSI Commission B and Sigma Xi. He was the recipient of the 1998 Erskine Fellowship with the University of Canterbury, Canterbury, New Zealand.

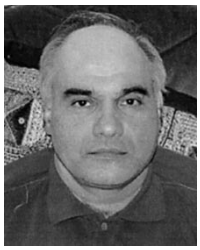

S. Safavi-Naeini (S'75–M'78) received the B.Sc. degree in electrical engineering from the University of Tehran, Tehran, Iran, 1974, and the M.Sc. and Ph.D. degrees in electrical engineering from the University of Illinois at Champaign-Urbana, in 1975 and 1979, respectively.

From 1980 to 1995, he was an Assistant Professor and then an Associate Professor with the Electrical Engineering Department, University of Tehran. Since 1996, he has been an Associate Professor with the Department of Electrical and Computer Engineering, University of Waterloo, Waterloo, ON, Canada. He has authored or coauthored over 110 papers in technical journals and conferences. He has been a scientific and technical consultant to a number of national and international telecom industrial and research organizations over the last 20 years. His research interests and activities include numerical electromagnetics applied to analysis and design optimization of RF/microwave/millimeter-wave systems and circuits, antenna and propagation, wireless communication systems, very high-speed digital circuits, and photonics.